RSC Advances

Synthesis and characterization of Zr-doped LiNi0.4Co0.2Mn0.4O2 cathode materials for lithium ion battery

Journal:	*RSC Advances*
Manuscript ID:	RA-ART-07-2015-014376.R1
Article Type:	Paper
Date Submitted by the Author:	19-Aug-2015
Complete List of Authors:	Chen, QiYuan; Tianjin University, Chemical Engineering; Tianjin University, Applied Chemistry Du, Chenqiang; Tianjin University, Applied Chemistry Qu, Deyang; McNair Technology Company, Limited, Zhang, Xinhe; McNair Technology Company, Limited, Tang, Zhiyuan; Tianjin University, Applied Chemistry

SCHOLARONE™
Manuscripts

Journal Name

ARTICLE

Synthesis and characterization of Zr-doped LiNi$_{0.4}$Co$_{0.2}$Mn$_{0.4}$O$_2$ cathode materials for lithium ion battery

QiYuan Chen,^{a*} Chenqiang Du,^{b} Deyang Qu,^{c} Xinhe Zhang^{c} and Zhiyuan Tang,^{b**}

Li(Ni$_{0.4}$Co$_{0.2}$Mn$_{0.4}$)$_{1-x}$Zr$_x$O$_2$(x=0,0.01) was synthesized by typical sol-gel method. The morphology, structure and electrochemical properties were characterized by SEM, XRD, charge-discharge tests, Cyclic Voltammetry (CV) and electrochemical impedance spectroscopy (EIS). The X-ray diffraction patterns showed that the substituted elements slightly enlarged the interlayer spacing and obtained higher degree of well-ordered crystallographic form. The doped sample Li(Ni$_{0.4}$Co$_{0.2}$Mn$_{0.4}$)$_{0.99}$Zr$_{0.01}$O$_2$ delivered a good electrochemical properties. The initial discharge capacities were 162.4 mAh g^{-1}, 157.5 mAh g^{-1}, 135.3 mAh g^{-1}, 124.3 mAh g^{-1} at 0.2 C, 0.5 C, 1.0 C and 2.0C, respectively. After 50 cycles, the capacity retentions were 80.5%, 70.9%, 73.4% and 68.5% at the corresponding rates, respectively. The improved electrochemical performance could be ascribed to enhanced diffusion rate of Li$^+$ and improved crystal structure.

1. Introduction

Lithium ion battery (LIBs) has served as the promising power sources for electric vehicles(EV) and hybrid electric vehicles (HEVs) due to their high energy and high power density.[1-3] Cathode materials are the most important components and receive a great attention since the LiMO$_2$ (M=Co, Ni) was proposed by J.B. Goodenough.[4] Currently, the most commonly used cathode material for Li-ion batteries is LiCoO$_2$ due to its high capacity, excellent cycle life, good rate capability, and high energy density. However, the material of LiCoO$_2$ only delivers a reversible capacity of 140 mAh g^{-1} due to the degradation of the crystal structure caused by the dislocation of lattice oxygen at high temperatures and at overcharged state of 4.2 V.[5,6] Besides, high cost and lack of resource of Co element limit the application of lithium-ion batteries. While, LiNiO$_2$ and LiMnO$_2$ cathode materials, as the Co-free alternatives, still suffer from their own imperfection. LiNiO$_2$ is difficult to be synthesized, and its unstable structure leads to rapid capacity fading and weak thermal stability.[7-9] LiMnO$_2$ is structurally unstable at high temperatures and is subject to severe capacity fading, which is surely ascribable to the irreversible transition to a spinel-like structure and is the primary obstacle to its applications in practice.[10-12] Thus,

searching for more suitable alternative cathode materials is necessary. LiNi$_{0.33}$Mn$_{0.33}$Co$_{0.33}$O$_2$, a novel kind of layered structure cathode material, which has all advantages of LiCoO$_2$, LiNiO$_2$ and LiMnO$_2$, has been developed by T. Ohzuku.[13,14] Its derivatives LiNi$_x$Co$_y$Mn$_{1-x-y}$O$_2$ (0⩽x, y, x+y⩽1) is a promising energy material on account of its high specific capacity and moderately high rate performance with stable structure and good safety property.[15-18] Nevertheless, there still exist some defects such as undesirable ionic conductivity, poor cycle performance and complicated preparation technique, which all affect its electrochemical performance and limit its commercialization.[19,20] Thus, various kinds of strategies are investigated to modify this layer cathode material, including surface coating [21,22] and ion doping [23,24]. Surface coating can protect active material from electrolyte, with reduction of the side reaction between active material and electrolyte, and then elevate the cycle ability, such as Ta$_2$O$_5$[25], TiO$_2$, ZrO$_2$, Al$_2$O$_3$,[26] Li$_3$VO$_4$[27], Li$_2$ZrO$_3$[28]-coating. However, surface coatings depress the specific energy and may introduce some new side reactions, which also limit its application. Comparing with coating methods, ion doping can modify the valence states of both transition metals and oxygen with charge compensation mechanisms that enhances the electronic conductivity of the host structure. In addition, it has been shown that the doped material remains single phase throughout the charge-discharge cycles, and thus its stability towards the electrolyte is increased. Therefore, various ion doping, such as Mg^{2+},Cr^{3+},Al^{3+},Y^{3+} has been used to stabilize the structure of layered cathode materials, then improve the capacity and cycling performance.[23,24,29,30] While Zr^{4+} has a bigger radius (0.72 A˚) than that of Ni^{2+} (0.69 A˚), it can serve as the pillar of layered structure to improve the structure

$^{a.}$ Department of Chemical Engineering, School of Chemical Engineering and Technology, Tianjin University, Tianjin 300072,China
$^{b.}$ Department of Applied Chemistry, School of Chemical Engineering and Technology, Tianjin University, Tianjin 300072, China
$^{c.}$ McNair Technology Company, Limited, Dongguan City, Guangdong 523700, China

stability and impede monoclinic distortion efficiently. However, there appears few reports about Zr^{4+} doped layer cathode material.

In this study we synthesized the Zr-doped $LiNi_{0.4}Co_{0.2}Mn_{0.4}O_2$ and investigated the structure, morphology and electrochemical performance of it. Besides, the pure $LiNi_{0.4}Co_{0.2}Mn_{0.4}O_2$ was also synthesized as a contrast. It was expected that the Zr-doped materials could obtain more ordered lamellar structure, less Li^+/Ni^{2+} mixing and better Li^+ transportation kinetics.

2. Experimental

2.1 Material preparation

$Li(Ni_{0.4}Co_{0.2}Mn_{0.4})_{1-x}Zr_xO_2$ (x=0,0.01) were prepared by a sol-gel method using citric acid as chelating agent and stoichiometric amounts of $CH_3COOLi\ 2H_2O$, $(CH_3COO)_2Ni\ 4H_2O$, $(CH_3COO)_2Mn\ 4H_2O$, $(CH_3COO)_2Co\ 4H_2O$ and $Zr(NO_3)_4\ 4H_2O$ as starting materials. The molar ratio of citric acid and metal acetate was 1:1. All of the reactants were analytical grade and used without further treatment. Firstly, all the reactants were dissolved in de-ionized water and mixed thoroughly. Then the mixture solution was transferred into a water bath and heated at 80 °C under vigorously stirring until a gel formed. The gel was dried in an oven at 80 °C for 12h and heated at 450 °C for 5 h in air atmosphere to allow a pyrolysis process. After grinding completely in a mortar, the precursor was calcined at 800 °C for 12 h in air atmosphere. As a result, the $Li(Ni_{0.4}Co_{0.2}Mn_{0.4})_{0.99}Zr_{0.01}O_2$ was obtained. As comparison, pure $LiNi_{0.4}Co_{0.2}Mn_{0.4}O_2$ was prepared under the same condition without adding Zr-source.

2.2. Materials characterization and Electrochemical measurements

The powder X-ray diffraction measurement was employed at 4°/min with the 2θ range of 10°~80°using Cu K_α radiation to examine the crystalline properties of the samples. The morphology and particle size distribution of both the pristine and the doped sample were observed using a scanning electron microscope (SEM) measurement with accelerating voltage of 3.0kV.

The active material was mixed with 10% conductive agent (super P), 10% binder agent (PVDF) and dissolved in the N-methyl pyrrolidone (NMP) to make a slurry. The slurry was coated on the aluminium foil, dried at 120 °C overnight and pressed with 10 MPa. The resulting cathode had an active material loading of about 2.8~3.0 mg cm^{-2}. The cells were assembled in an argon-filled glove box with the moisture content and oxygen level less than 5 ppm. Metallic lithium foils served as counter and reference electrodes. The electrolyte was 1M $LiPF_6$ in a mixture of ethylene carbonate and dimethyl carbonate (1:1 in volume). Galvanostatic charge and discharge tests were performed between 2.6 V and 4.7 V at room temperature on a battery test system (LISUN- CBT-
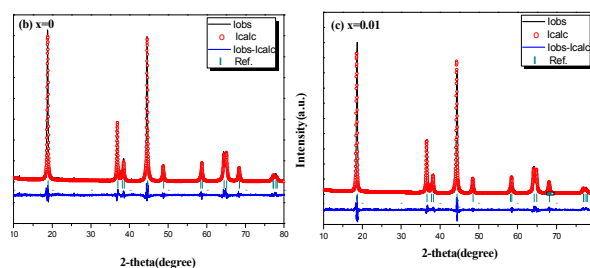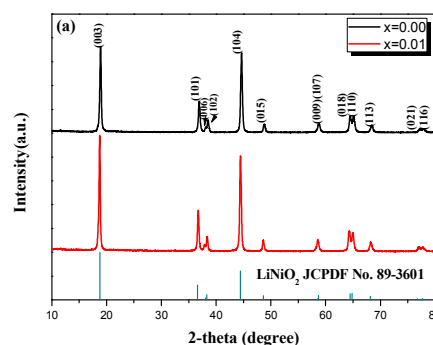

Fig.1. X-ray diffraction patterns (a) and Rietveld refinement (b, c) of the $Li(Ni_{0.4}Co_{0.2}Mn_{0.4})_{1-x}Zr_xO_2$ (x=0, 0.01) powders.

Table .1 Lattice parameters of $Li(Ni_{0.4}Co_{0.2}Mn_{0.4})_{1-x}Zr_xO_2$ samples.

138-32). Cyclic voltammetry test was carried out at a scanning

Sample	Lattice parameters				intensity ratio	interlayer space
	a(Å)	c(Å)	c/a	$V_0(Å^3)$	$I_{(003)}/I_{(104)}$	d_{003}(Å)
x=0.00	2.866	14.241	4.967	101.30	1.25	4.738
x=0.01	2.871	14.271	4.970	102.08	1.31	4.795

rate of 0.1 mV s^{-1} between 2.6 V and 4.8 V on an electrochemical workstation (ChenHua CHI1040B, China). And the electrochemical impedance spectroscopy (EIS) analysis was carried out by applying an AC voltage of 5 mV over the frequency range from 100 kHz to 10 mHz on an electrochemical workstation (Gamry PC14-750, USA). All electrical measurements had been performed at room temperature.

3. Results and discussion

3.1 Structure and morphology analysis

Fig 1 has shown the X-ray diffraction patterns of the $Li(Ni_{0.4}Co_{0.2}Mn_{0.4})_{1-x}Zr_xO_2$ (x=0,0.01) powders. All the diffraction peaks are indexed on the basis of hexagonal-$LiNiO_2$ structure with a space group of R3m (JCPDS card No. 89-3601), It seems
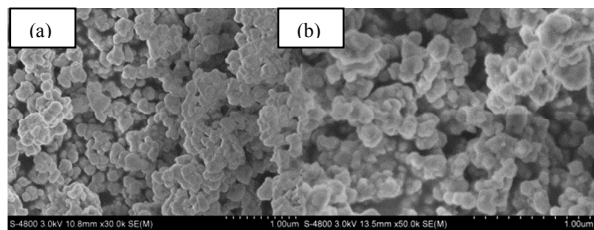
Fig.2.SEM images of Li(Ni$_{0.4}$Co$_{0.2}$Mn$_{0.4}$)$_{1-x}$Zr$_x$O$_2$ samples: (a)x=0, (b)x=0.01.

that there is no obvious difference between both samples in the XRD patterns, which indicates that partial metal-ionic substitution does not change the hexagonal layer structure. The clear split of the (006)/(102) and (108)/(110) doublets for the two samples indicates the formation of a well-ordered layer structure.[31,32] The structural analyses are conducted on the recorded XRD data based on Rietveld refinement. The calculated lattice parameters are listed on Tab.1. As shown in it, the lattice parameter d$_{003}$ represents the interlayer space on account of (003) peak. Obviously, Li(Ni$_{0.4}$Co$_{0.2}$Mn$_{0.4}$)$_{0.99}$Zr$_{0.01}$O$_2$ presents higher value of d$_{003}$ than that of un-doped one. Moreover, the value of c/a for Li(Ni$_{0.4}$Co$_{0.2}$Mn$_{0.4}$)$_{0.99}$Zr$_{0.01}$O$_2$ is larger than that of LiNi$_{0.4}$Co$_{0.2}$Mn$_{0.4}$O$_2$, which indicates a better layer structure in terms of statistics.[33] The integrated intensity ratio of (003)/(104) can be considered as a good measurement of cation mixing, which results from the interchange of lithium ions located in 3a sites and the transition metal ions occupied in 3b sites due to the similarity of their ionic radii.[34] From the tabulated data, it can be clearly seen that the introduction of Zr^{4+} can reduce the cation inter-mixing and stabilize the structure. Furthermore，the unit cell volume of Li(Ni$_{0.4}$Co$_{0.2}$Mn$_{0.4}$)$_{0.99}$Zr$_{0.01}$O$_2$ is larger than that of LiNi$_{0.4}$Co$_{0.2}$Mn$_{0.4}$O$_2$, which should be ascribed to the introduction of larger radius of Zr^{4+} in the LiNi$_{0.4}$Co$_{0.2}$Mn$_{0.4}$O$_2$. The bigger ionic radii of Zr^{4+} brings about the larger space for diffusion during Li$^+$ insertion and desertion process, which can enhance the electrochemical properties effectively. The SEM images of Li(Ni$_{0.4}$Co$_{0.2}$Mn$_{0.4}$)$_{0.99}$Zr$_{0.01}$O$_2$ and LiNi$_{0.4}$Co$_{0.2}$Mn$_{0.4}$O$_2$ are shown in Fig.2. There exist small agglomerates for both the powders. All primary particles show aspheric shape and a narrow particle size distribution ranging from 100 nm to 300 nm. There is no large morphological change between the bare LiNi$_{0.4}$Co$_{0.2}$Mn$_{0.4}$O$_2$ and the doped Li(Ni$_{0.4}$Co$_{0.2}$Mn$_{0.4}$)$_{0.99}$Zr$_{0.01}$O$_2$, which demonstrates that Zr^{4+} doping does not obviously affect the morphology of the target products. Besides, the doped powder displays a slightly smaller value of average particle size in comparison with that of the bare sample, which is favourable for shortening the diffusion path of Li$^+$ and thus improving the electrochemical performance.

3.2 Electrochemical behaviours

Fig 3. shows the CV curves of Li(Ni$_{0.4}$Co$_{0.2}$Mn$_{0.4}$)$_{0.99}$Zr$_{0.01}$O$_2$ and LiNi$_{0.4}$Co$_{0.2}$Mn$_{0.4}$O$_2$ between 2.6 V and 4.8 V for the first three cycles at the scanning rate of 0.1 mV s^{-1}. As shown in Fig.3, the

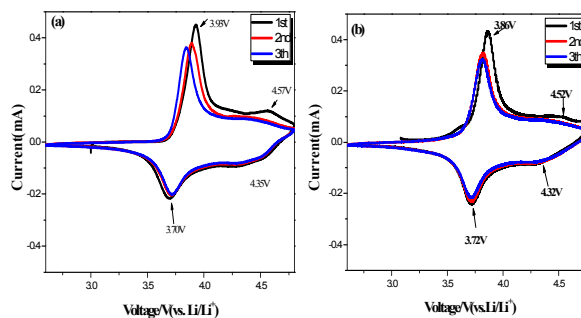**Fig.3**.Cyclic Voltammogram of Li(Ni$_{0.4}$Co$_{0.2}$Mn$_{0.4}$)$_{1-x}$Zr$_x$O$_2$ samples at 0.1mVs^{-1} between 2.6-4.8V for the first three cycles.(a)x=0; (b)x=0.01.

Table 2 the oxidation peak potential (E$_{pa}$), reduction peak potential (E$_{pc}$) and the corresponding difference obtained from CV curves of Li(Ni$_{0.4}$Co$_{0.2}$Mn$_{0.4}$)$_{1-x}$Zr$_x$O$_2$ for the first three cycles.

Value	x=0			x=0.01		
(V, vs. Li/Li$^+$)	1st	2nd	3th	1st	2nd	3th
E$_{pa}$	3.928	3.893	3.844	3.864	3.820	3.818
E$_{pc}$	3.697	3.711	3.717	3.719	3.715	3.714
ΔE=E$_{pa}$-E$_{pc}$	0.231	0.182	0.127	0.145	0.105	0.104
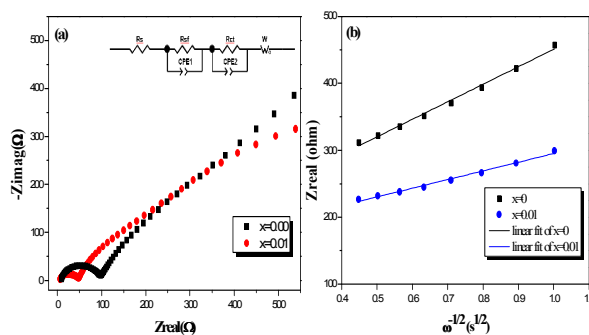
Fig.4 Nyquist plots (a) and the plots of Z$_{real}$ as a function of ω$^{-1/2}$ (b) of Li(Ni$_{0.4}$Co$_{0.2}$Mn$_{0.4}$)$_{1-x}$Zr$_x$O$_2$ (x=0,0.01) samples after 1st cycle under rate of 1.0C. Inset is equivalent circuit model simulated to give related parameters.

relative broad peaks between 3.7 V and 4.7 V on the charge curves are ascribed to the oxidation of Ni ions (Ni^{2+}→Ni^{4+}) and Co ions (Co^{3+}→Co^{4+}), accounting for the Li$^+$ extraction from the NCM component.[35] The reduction peak around 3.7 V was observed on the discharge curve, illustrating the reduction of Ni ions (Ni^{4+}→Ni^{2+}) and Co ions (Co^{4+}→Co^{3+}), which means Li$^+$ inserts back into the NCM layered material. As shown in Tab.2, the potential differences between cathodic and anodic peaks of Li(Ni$_{0.4}$Co$_{0.2}$Mn$_{0.4}$)$_{0.99}$Zr$_{0.01}$O$_2$ is less than that of LiNi$_{0.4}$Co$_{0.2}$Mn$_{0.4}$O$_2$, which indicates that Zr^{4+} doping enhance the ionic conductivity, weaken the polarization of the cell and thus improve cycle reversibility of as-prepared electrode.

Table.3 the obtained resistance parameters from simulation of elements in equivalent circuit model.

Sample	R_s (Ω cm^{-2})	R_{SEI} (Ω cm^{-2})	CPE1 (10^{-5} S cm^2)	R_{ct} (Ω cm^{-2})	CPE2 (10^{-2} S cm^2)
x=0.00	9.846	81.02	0.602	173.9	0.903
x=0.01	7.883	38.86	1.37	95.98	1.03

Fig.5. Initial charge-discharge curves (a), cycling curves (b) and rate performance (c) of Li(Ni$_{0.4}$Co$_{0.2}$Mn$_{0.4}$)$_{1-x}$Zr$_x$O$_2$ (x=0,0.01) samples between 2.6-4.7V.

Electrochemical impedance spectroscopy (EIS) is found to be a useful tool to evaluate the electronic conductivity and lithium-ion diffusion coefficient of the as-prepared materials[36] and is utilized to analyze the electrochemical kinetics of Li(Ni$_{0.4}$Co$_{0.2}$Mn$_{0.4}$)$_{1-x}$Zr$_x$O$_2$ (x=0,0.01). As shown in Fig.4 (a), the Nyquist plots of the cells consist of two semicircles alike in the high and intermediate frequency ranges and a straight line with total changing slope to the real axes (in the lower frequency range). Generally, an intercept at the Z_{real} axis at a high frequency range corresponds to the ohmic resistance (R_s), which represents the resistance of the electrolyte, separator, and electrical contacts. The depressed semicircle in the high frequency domain is related to the Li-ion migration resistance (R_{SEI}) through the SEI film formed on the electrode. The second semicircle in the middle frequency range indicates the charge transfer resistance (R_{ct}). The inclined line in the lower frequency range represents the Warburg impedance and corresponds to the lithium diffusion kinetics towards the electrodes. The study of the EIS results has been performed by using the approach outlined in Ref. [37-39] by using an equivalent circuit model shown in upper right corner inset of Fig. 4(a). The fitting results derived from the equivalent circuit are presented in Tab.3. As shown in it, the electrolyte resistance remains almost constant, which is expected since the variation of an electrolyte concentration is not so large to affect the electrolyte conductivity. The Li-ion migration resistance (R_{SEI}) and charge transfer resistance (R_{ct}) of Li(Ni$_{0.4}$Co$_{0.2}$Mn$_{0.4}$)$_{0.99}$Zr$_{0.01}$O$_2$ is smaller than those of LiNi$_{0.4}$Co$_{0.2}$Mn$_{0.4}$O$_2$. Because growth in surface film resistance leads to the capacity loss during cycling and the change of charge transfer resistance is mainly ascribed to the total resistance change during discharging[40], the major depression in R_{SEI} and R_{ct} of the doped sample fully expresses minor Zr^{4+} doping improves the kinetic behaviour of Li$^+$ intercalation/de-intercalation process, and thus achieves better electrochemical performances.

In order to clarify the effect of Zr^{4+}-doping on the Li$^+$ conductivity of LiNi$_{0.4}$Co$_{0.2}$Mn$_{0.4}$O$_2$ material, lithium-ion diffusion coefficient D_{Li}^+ could be obtained from the slope in the low frequency according to the following equation:[41]

$$D_{Li} = \frac{R^2 T^2}{2A^2 F^4 n^4 C^2 \sigma^2}$$

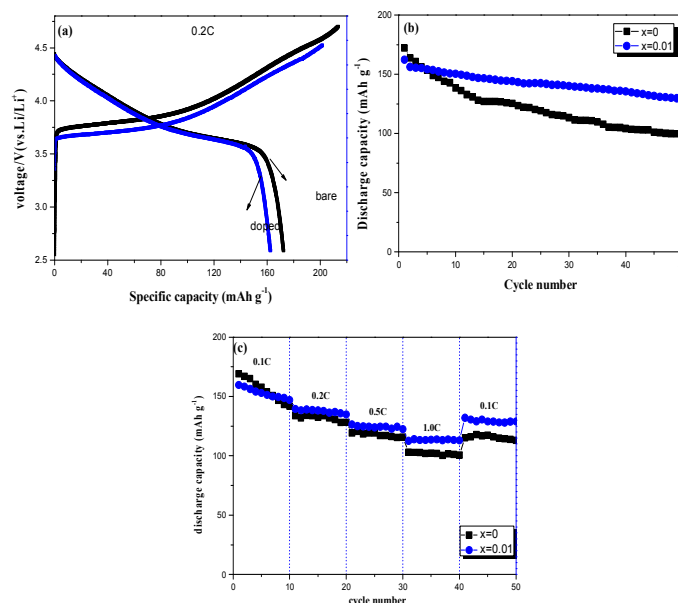Here, R is the gas constant (R=8.314 J mol^{-1} k^{-1}), T is the absolute temperature (T=298.15 K), A is related to the cathode surface area (A=0.785 cm^2), n is the number of electrons per molecule during oxidization (n=1), F is the Faraday constant (F=96485.34 C mol^{-1}), C is the lithium-ion concentration, which can be obtained from lattice parameter V$_0$,[42] and σ refers to the Warburg factor. The Warburg factor can be calculated according to the following equation:

$$Z_{real} = R_{SEI} + R_{CT} + \sigma\omega^{-1/2}$$

Here, ω is the low frequency. Fig.4 (b) illustrates the relationship between Z_{real} and $\omega^{-1/2}$ in the low frequency region. According to the above two equations, we can calculate the value of σ and D_{Li}^+, which are 129.5Ω s$^{-1/2}$ and 1.44×10^{-11}cm^2 s^{-1}, 261.9Ω s$^{-1/2}$ and 3.45×10^{-12}cm^2 s^{-1} for Li(Ni$_{0.4}$Co$_{0.2}$Mn$_{0.4}$)$_{0.99}$Zr$_{0.01}$O$_2$, LiNi$_{0.4}$Co$_{0.2}$Mn$_{0.4}$O$_2$, respectively. Thus, minor Zr^{4+}-doping improves the diffusion rate of Li$^+$ apparently, which is advantageous to the rate performance. Fig.5 illustrates the initial charge-discharge curves, cycling curves and rate performance of Li(Ni$_{0.4}$Co$_{0.2}$Mn$_{0.4}$)$_{1-x}$Zr$_x$O$_2$ (x=0,0.01) at 0.2C between 2.6 V and 4.7 V at room temperature. As shown in Fig.5 (a), LiNi$_{0.4}$Co$_{0.2}$Mn$_{0.4}$O$_2$ delivers the initial charge and discharge capacities of 215.3mAh g^{-1} and 172.2 mAh g^{-1} at 0.2C, respectively. While the initial charge and discharge capacities of Li(Ni$_{0.4}$Co$_{0.2}$Mn$_{0.4}$)$_{0.99}$Zr$_{0.01}$O$_2$ are 201.4mAh g^{-1} and 162.4mAh g^{-1} at the corresponding discharge rate. The slightly reduced initial discharge capacity of Li(Ni$_{0.4}$Co$_{0.2}$Mn$_{0.4}$)$_{0.99}$Zr$_{0.01}$O$_2$ should be attribute to lower amount of Ni^{2+} resulted from the substitution of Zr^{4+}. Fig.5 (b) displays the cycling curves of Li(Ni$_{0.4}$Co$_{0.2}$Mn$_{0.4}$)$_{1-x}$Zr$_x$O$_2$ at 0.2C. Li(Ni$_{0.4}$Co$_{0.2}$Mn$_{0.4}$)$_{0.99}$Zr$_{0.01}$O$_2$ delivers the discharge capacities of 135.1mAh g^{-1} after 50 cycles and keeps the capacity retention of 80.5%, which are both larger than those of
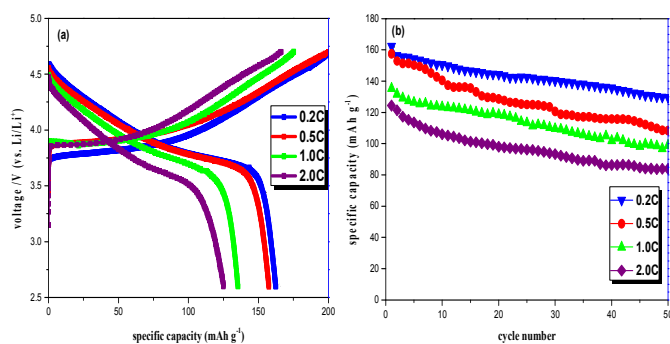
Fig.6 Initial charge/discharge curves (a) and cycle performance (b) of Li(Ni$_{0.4}$Co$_{0.2}$Mn$_{0.4}$)$_{0.99}$Zr$_{0.01}$O$_2$ samples at different rates between 2.6-4.7V.

LiNi$_{0.4}$Co$_{0.2}$Mn$_{0.4}$O$_2$. Additionally, the rate performance for both Li(Ni$_{0.4}$Co$_{0.2}$Mn$_{0.4}$)$_{0.99}$Zr$_{0.01}$O$_2$ and LiNi$_{0.4}$Co$_{0.2}$Mn$_{0.4}$O$_2$ is also revealed in Fig.5(c) with the discharge rates increasing from 0.1C in steps to 1.0C, each rate for 10 cycles, and 0.1C in the last round. The discharge rate keeps 0.1C to ensure the comparability of results. Although the capacities at the initial cycles for the doped sample is slightly lower than those of the un-doped one, they fade slower with the increasing discharge rates. And it can be clearly seen that Li(Ni$_{0.4}$Co$_{0.2}$Mn$_{0.4}$)$_{0.99}$Zr$_{0.01}$O$_2$ delivers more capacity at large rates and the difference is enlarged with the growing rate. Obviously, zirconium-doping improves the cycling stability and rate capability of LiNi$_{0.4}$Co$_{0.2}$Mn$_{0.4}$O$_2$ at the same time. This phenomenon can be elucidated by the fact that the substituted ions located at TM (transition metal) layer can prevent the local structure collapse during lithium ions desertion/insertion process.[43,44]

To further investigate the electrochemical behaviours of Li(Ni$_{0.4}$Co$_{0.2}$Mn$_{0.4}$)$_{0.99}$Zr$_{0.01}$O$_2$, the rate performance and cycle ability are investigated. As shown in Fig.6 (a), the initial discharge capacities of Li(Ni$_{0.4}$Co$_{0.2}$Mn$_{0.4}$)$_{0.99}$Zr$_{0.01}$O$_2$ are 162.4 mAh g^{-1}, 157.5 mAh g^{-1}, 135.3 mAh g^{-1}, 124.3 mAh g^{-1} at 0.2 C, 0.5 C, 1.0 C and 2.0C, respectively. After 50 cycles, the Li(Ni$_{0.4}$Co$_{0.2}$Mn$_{0.4}$)$_{0.99}$Zr$_{0.01}$O$_2$ still delivers 130.7 mAh g^{-1}, 111.7 mAh g^{-1}, 99.3 mAh g^{-1} and 85.1 mAh g^{-1} at the corresponding rates, and the capacity retention are 80.5%, 70.9%, 73.4% and 68.5% respectively. As a result, the Zr^{4+}-doping should be an effective way to improve the cycling stability of LiNi$_{0.4}$Co$_{0.2}$Mn$_{0.4}$O$_2$ cathode material.

Conclusions

Li(Ni$_{0.4}$Co$_{0.2}$Mn$_{0.4}$)$_{1-x}$Zr$_x$O$_2$ was successfully prepared via sol-gel method. The structure, morphology and electrochemical performance of Li(Ni$_{0.4}$Co$_{0.2}$Mn$_{0.4}$)$_{0.99}$Zr$_{0.01}$O$_2$ and LiNi$_{0.4}$Co$_{0.2}$Mn$_{0.4}$O$_2$ are investigated. The results show that Li(Ni$_{0.4}$Co$_{0.2}$Mn$_{0.4}$)$_{0.99}$Zr$_{0.01}$O$_2$ has a well-crystallized structure and aspheric morphology with particle size of 100~300 nm. Meanwhile, comparing with LiNi$_{0.4}$Co$_{0.2}$Mn$_{0.4}$O$_2$,

Li(Ni$_{0.4}$Co$_{0.2}$Mn$_{0.4}$)$_{0.99}$Zr$_{0.01}$O$_2$ displays better electrochemical performances. The initial discharge capacities of the doped sample are 162.4 mAh g^{-1}, 157.5 mAh g^{-1}, 135.3 mAh g^{-1}, 124.3 mAh g^{-1} at 0.2 C, 0.5 C, 1.0 C and 2.0C, and the corresponding capacity retentions after 50 cycles are 80.5%, 70.9%, 73.4% and 68.5%, respectively. Therefore, Zr^{4+} tends to be a good candidate in ion doping materials to enhance the electrochemical performance of layered cathode materials.

Acknowledgements

Notes and references

1   J. Hassoun, K.S. Lee, Y.K. Sun and B. Scrosati, *J. Am. Chem. Soc*, 2011, **133**, 139.
2   J.B. Goodenough and K-S Park, *J. Am. Chem. Soc*, 2013, **135**, 1167.
3   J.B. Goodenough, and Y. Kim, *Chem. Mater*, 2010, **22**, 587.
4   K. Mizushima, P.C. Jones, P.J. Wiseman and J.B. Goodenough, *Mater. Res. Bull*, 1980, **15**, 783.
5   E.I. Santiago, A.V.C. Andrade, C.O. Paiva-Santos and L.O.S. Bulho˜es, *Solid State Ionics,* 2003, **158**, 91.
6   B. Huang, Y-I. Jang, Y-M. Chiang and D. R. Sadoway, *Journal of Applied Electrochemistry*, 1998, **28**, 1365.
7   P. Kalyani and N. Kalaiselvi, *Science and Technology of Advanced Materials,* 2005, **6**, 689.
8   Hajime Arai, Shigeto Okada, Yoji Sakurai and Jun-ichi Yamaki, *Solid State Ionics*, 1997, **95**, 275.
9   Jaephil Cho, HyunSook Jung, YoungChul Park, GeunBae Kim, and Hong Sup Lim, *Journal of The Electrochemical Society*, 2000, **147**, 15.
10 R. J. Gummow and M. M. Thackeray, *J. Electrochem. Soc*, 1994, **141**, 1178.
11 Z.F. Huang, X. Meng, C.Z. Wang, Y. Sun and G. Chen, *J. Power Sources*, 2006, **158**, 1394.
12 Y. Koyama, Y. Makimura, T. Ohzuku, H. Adachi and T. Uhuru, *J. Electrochem.Soc*, 2004, **151**, A1499.
13 T. Ohzuku and Y. Makimura, *Chem. Lett*., 2001, **7**, 642.
14 N. Yabuuchi and T. Ohzuku, *J. Power Sources*, 2003, **119**, 171.
15 J. Zheng, W.H. Kan and A. Manthiram, *ACS Appl. Mater. Interfaces*, 2015, **7**, 6926.
16 S.T.Sun, C.Q. Du, D.Y. Qu, X.H. Zhang and Z.Y. Tang, *Ionics*, 2015, **21**, 2091.
17 K. Chen, Y. Shen, J. Jiang, Y. Zhang, Y. Lin and C.W. Nan, *J. Mater. Chem. A*, 2014, **2**, 13332.
18 C.H. Jo, D.H. Cho, H.J. Noh, H. Yashiro, Y.K. Sun and S.T. Myung, *Nano Research*, 2015, **8**, 1464.
19 K.C. Kam and M.M. Doeff, *J. Mater. Chem*, 2011, **21**, 9991.
20 Y. Cho, P. Oh and J. Cho, *Nano Lett*, 2013, **13**, 1145.
21 L. A. Riley, S.V. Atta, A. S. Cavanagh, Y.F Yan, S. M. George, P. Liu, A.C. Dillon and S.H. Lee, *J. Power Sources*, 2011, **196**, 3317.
22 F. Wu, Z. Wang, Y.F. Su, N. Yan, L.Y. Bao and S. Chen, *J. Power Sources*, 2014, **247**, 20.
23 G.H. Kim, S.T. Myung, H.S. Kim and Y.K. Sun, *Electrochim. Acta*, 2006, **51**, 2447.

24 J. Guo, L.F. Jiao, H.T. Yuan, L.Q. Wang, H.X. Li, M. Zhang and Y.M. Wang, *Electrochim. Acta*, 2006, **51**, 6275.
25 X.F. Li, J. Liu, M. N. Banis, A. Lushington, R.Y. Li, M. Cai and X.L. Sun, *Energy Environ. Sci*, 2014, **7**, 768.
26 X.F. Li, J. Liu, X.B. Meng, Y.J. Tang, M. N. Banis, J.L. Yang, Y.H. Hu, R.Y. Li, M. Cai and X.L. Sun, *J. Power Sources*, 2014, **247**, 57.
27 W.L. Wang, Z.L. Yin, Z.X.Wang, X.H. Li and H.J. Guo, *Materials Letters*, 2015,**160**, 298.
28 D. Wang, X.H. Li, Z.X. Wang, H.J. Guo, Z.J. Huang, L.K. Kong and J.J. Ru, *Journal of Alloys and Compounds*, 2015, **647**, 612.
29 J. Bains, L. Croguennec, J. Bréger, F. Castaing, S. Levasseur, C. Delmas and Ph. Biensan, *J. Power Sources*, 2011, **196**, 8625.
30 M. Wang, Y.B. Chen, F. Wu, Y.F. Su, L. Chen and D.L. Wang, *Electrochimca. Acta*, 2010, **55**, 8815.
31 J.G. Li, L.Wang, Q. Zhang and X.M. He, *J. Power Sources*, 2009, **189**, 28.
32 H.B. Ren, Y.R. Wang, D.C. Li, L.H. Ren, Z.H. Peng and Y.H. Zhou, *J. Power Sources*, 2008, **178**, 439.
33 C. Nitthya, V.S. Syamala Kumari, S and Gopukumar, *Phys. Chem, Chem. Phys*, 2011, **13**, 6125.
34 M. Sathiya, A.S. Prakash, K. Ramesha and A.K. Shukla, *Mater. Res. Bull*, 2009, **44**, 1990.
35 Chien-Te Hsieh, Chung-Yu Mo, Yu-Fu Chen and Yi-Jou Chung, *Electrochimica Acta*, 2013, **106**, 525.
36 B. Yan, M.S. Li, X.F. Li, Z.M. Bai, J.W. Yang, D.B. Xiong and De.J. Li, *J. Mater. Chem. A*, 2015, **3**, 11773.
37 M. Yang, C.Q. Du, Z.Y. Tang, J.W. Wu and X.H. Zhang, *Ionics*, 2014, **20**, 1039.
38 C.Q. Du, J.W. Wu, J. Liu, M. Yang, Q. Xu, Z.Y. Tang and X.H. Zhang, *Electrochimca. Acta*, 2015, **152**, 473.
39 Y.Y. Li, C.Q. Du, J. Liu, F. Zhang, Q. Xu, D. Qu, X.H. Zhang and Z.Y. Tang, *Electrochimca. Acta*, 2015, **167**, 201.
40 B. Yan, M.S. Li, X.F. Li, Z.M. Bai, L. Dong, D.J. Li, *Electrochimica Acta*, 2015, **164**, 55
41 H.J. Noh, S. Youn, C.S. Yoon and Y.K. Sun, *J. Power Sources*, 2013, **233**, 121.
42 P. Gao, Y.H. Li, H.D. Liu, Jo. Pinto, X.F. Jiang, and G. Yang, *Journal of The Electrochemical Society*, 2012, **159 (4)**, A506.
43 P.B. Samarasingha, A. Wijayasinghe, M. Behm, L. Dissanayake and G. Lindbergh, *Solid State Ionics*, 2014, 1.
44 G. Singh, R. Thomas, A. Kumar and R. S. Katiyar. *Journal of The Electrochemical Society*, 2012, **159**, A410.